BBA - Molecular and Cell Biology of Lipids 1866 (2021) 158908

Contents lists available at ScienceDirect

BBA - Molecular and Cell Biology of Lipids

journal homepage: www.elsevier.com/locate/bbalip

Immunomodulating effects of 13- and 16-hydroxylated docosahexaenoyl ethanolamide in LPS stimulated RAW264.7 macrophages

Ian de Bus [a,b], Sandra van Krimpen [a], Guido J. Hooiveld [a], Mark V. Boekschoten [a], Mieke Poland [a], Renger F. Witkamp [a], Bauke Albada [b,*,1], Michiel G.J. Balvers [a,*,1]

[a] Division of Human Nutrition and Health, Wageningen University & Research, Stippeneng 4, 6708 WE Wageningen, the Netherlands
[b] Laboratory of Organic Chemistry, Wageningen University & Research, Stippeneng 4, 6708 WE Wageningen, the Netherlands

ARTICLE INFO

Keywords:
Docosahexaenoyl ethanolamide
Transcriptome
Immunomodulation
Cyclooxygenase
Endocannabinoid
Macrophage

ABSTRACT

Docosahexaenoyl ethanolamide (DHEA), the ethanolamine conjugate of the n-3 long chain polyunsaturated fatty acid docosahexaenoic acid, is endogenously present in the human circulation and in tissues. Its immunomodulating properties have been (partly) attributed to an interaction with the cyclooxygenase-2 (COX-2) enzyme. Recently, we discovered that COX-2 converts DHEA into two oxygenated metabolites, 13- and 16-hydroxylated-DHEA (13- and 16-HDHEA, respectively). It remained unclear whether these oxygenated metabolites also display immunomodulating properties like their parent DHEA. In the current study we investigated the immunomodulating properties of 13- and 16-HDHEA in lipopolysaccharide (LPS)-stimulated RAW264.7 macrophages. The compounds reduced production of tumor necrosis factor alpha (TNFα), interleukin (IL)-1β and IL-1Ra, but did not affect nitric oxide (NO) and IL-6 release. Transcriptome analysis showed that the compounds inhibited the LPS-mediated induction of pro-inflammatory genes (InhbA, Ifit1) and suggested potential inhibition of regulators such as toll-like receptor 4 (TLR4), MyD88, and interferon regulatory factor 3 (IRF3), whereas anti-inflammatory genes (SerpinB2) and potential regulators IL-10, sirtuin 1 (Sirt-1), fluticasone propionate were induced. Additionally, transcriptome analysis of 13-HDHEA suggests a potential anti-angiogenic role. In contrast to the known oxylipin-lowering effects of DHEA, liquid chromatography coupled to tandem mass spectrometry (LC-MS/MS) analyses revealed that 13- and 16-HDHEA did not affect oxylipin formation. Overall, the anti-inflammatory effects of 13-HDHEA and 16-HDHEA are less pronounced compared to their parent molecule DHEA. Therefore, we propose that COX-2 metabolism of DHEA acts as a regulatory mechanism to limit the anti-inflammatory properties of DHEA.

1. Introduction

Long chain n-3 polyunsaturated fatty acids (LC-PUFAs) are essential for neural development and functioning, and have been linked to certain beneficial health effects. For example, n-3 LC-PUFAs have been associated with neuroprotective and anti-depressant effects, improved endothelial functioning, lowered triglyceride levels, functional fetal and infant development, and proper cardiovascular and immune functioning [1–3]. Moreover, n-3 LC-PUFAs are described to inhibit propagation of many (chronic) inflammatory diseases like inflammatory bowel disease [4], cardiovascular disease [5,6], rheumatoid arthritis [7–9], and asthma [10]. Notwithstanding this, the potential health effects of n-3 LC-PUFAs are continuously being challenged by new studies. Suggested explanations for these apparent discrepancies are differences in the level of intake or administered dose, and the study population [1].

One of the most studied n-3 LC-PUFAs is docosahexaenoic acid (DHA; C22:6-n3). DHA exerts immunomodulating effects through various mechanisms [1]. First, DHA can directly bind to receptors or key regulators of inflammatory processes [11], such as peroxisome proliferator-activated receptor gamma (PPARγ) [12] or the G-protein coupled receptor 120 (GPR120) [13,14]. Second, increased dietary DHA intake alters the cell membrane composition leading to a higher n-3 content. This change in membrane composition leads to a decreased production of pro-inflammatory n-6 oxylipins and increases the production of potent inflammation resolving n-3 oxylipins including resolvins, protectins, and maresins [1,11,15–19]. Third, DHA is

* Corresponding authors.
E-mail addresses: bauke.albada@wur.nl (B. Albada), michiel.balvers@wur.nl (M.G.J. Balvers).
[1] Both authors contributed equally to this manuscript.

https://doi.org/10.1016/j.bbalip.2021.158908
Received 2 November 2020; Received in revised form 23 January 2021; Accepted 15 February 2021
Available online 19 February 2021

converted to the endocannabinoid-like structure docosahexaenoyl ethanolamide (DHEA) (Fig. 1). DHEA is endogenously present in the circulation and tissues in humans and animals [15,20–25], and its levels are generally increased after DHA intake, for example by consumption of n-3 fatty acid-containing products such as fatty fish or fish oil supplements [15,20,22,26]. Although the exact biosynthetic route of DHEA is yet to be determined, evidence suggests the involvement of *N*-acyl transferase and *N*-acyl phosphatidylethanolamine-specific phospholipase D (NAPE-PLD) [27,28]. Breakdown of DHEA is subsequently mediated by fatty acid amide hydrolase (FAAH) (Fig. 1) [28]. Importantly, DHEA is a potent inhibitor of inflammation in various models [1,28,29]. For example, DHEA inhibits neuroinflammation *via* interaction with the GPR110 [28,30], and reduces the production of inflammation markers like monocyte chemoattractant protein 1 (MCP-1), NO, IL-6, and prostaglandin E_2 (PGE_2) in LPS-stimulated RAW264.7 macrophages and 3T3-L1 adipocytes [1,29,31–33].

DHEA can be oxygenated to form DHEA derived metabolites with novel biological activities [1,34]. Previously, 15-lipooxygenase (15-LOX) was shown to metabolize DHEA into 17-hydroxydocosahexaenoyl ethanolamide (17-HDHEA), which is further metabolized into 10,17-dihydroxydocosahexaenoyl ethanolamide (10,17-diHDHEA), 15-hydroxy-16(17)-epoxy-docosapentaenoyl ethanolamide (15-HEDPEA), and 13-HEDPEA. Of those metabolites, 10,17-diHDHEA and 15-HEDPEA prevented formation of platelet-leukocyte aggregates in human whole blood, and 15-HEDPEA possessed organ protecting roles in mouse reperfusion second organ injury [35]. CYP450-derived epoxide metabolites of DHEA were also shown to possess anti-inflammatory, anti-angiogenic, anti-migratory, and antitumorigenic properties [36,37]. Collectively, these data underline that DHEA is not a terminal end product of DHA, and that its oxygenated metabolites display a variety of immunomodulatory properties.

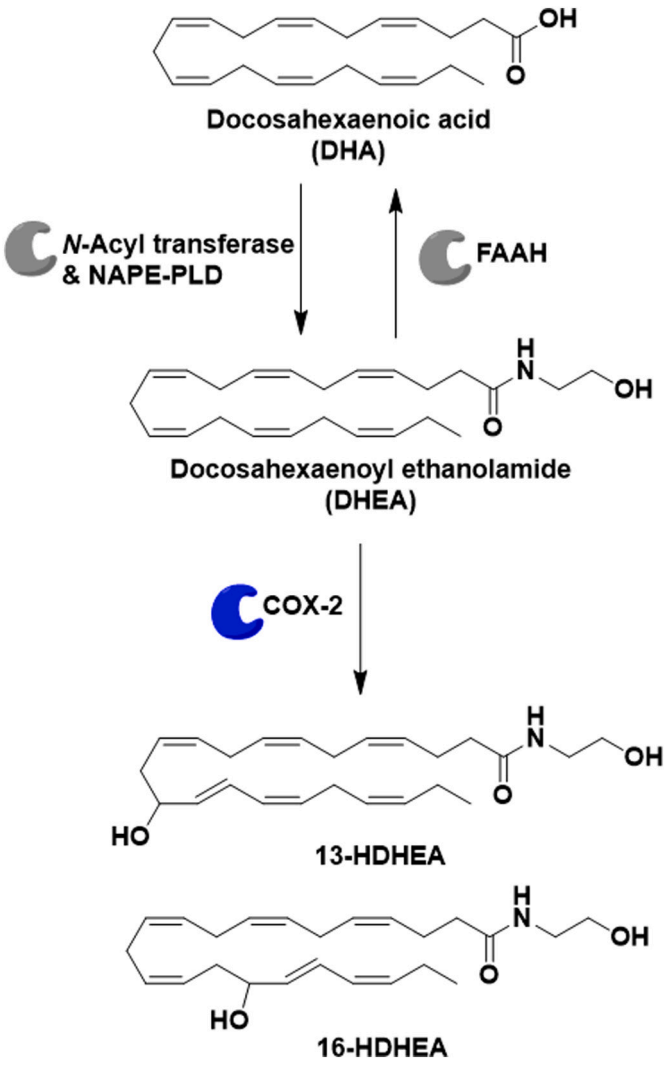

Fig. 1. Overview of the COX-2 mediated synthesis of 13-HDHEA and 16-HDHEA from DHEA, including the suggested synthesis of DHEA from DHA involving *N*-acyl transferase and NAPE-PLD. Hydrolysis of DHEA to DHA is mediated by FAAH.

Recently, we showed that COX-2 also metabolizes DHEA. Using enzyme assays, we demonstrated that purified COX-2 converts DHEA into 13- and 16-HDHEA, and we confirmed its formation in 1.0 μg/mL LPS-stimulated RAW264.7 macrophages (Fig. 1) [38]. Because of the observed immunomodulatory properties of the various oxygenated DHEA metabolites, it is tempting to speculate that 13- and 16-HDHEA also exert biological effects. To determine if this is the case, we performed a series of studies to unravel the immunomodulating properties of 13- and 16-HDHEA in comparison to their parent DHEA. In the current work, we analyzed the biological effects of the compounds on individual cytokine level using ELISAs. Subsequently, we measured effects on mRNA expression levels in RAW264.7 macrophages using transcriptomic analysis. Finally, we screened the production of lipid mediators from several selected enzymes using targeted metabolomics with LC-MS/MS.

2. Materials and methods

2.1. Materials

DHEA (≥98%), (±)13-HDHA (≥98%), (±)16-HDHA (≥98%), 5-HETE (≥95%), 5-HETE-d_8 (≥99% deuterated forms (d_1-d_8)), LTB_4 (≥97%), LTC_4 (≥97%), LTD_4 (≥97%), LTD_4-d_5 (≥99% deuterated forms (d_1-d_5)), PGE_2 (≥98%), PGD_2 (≥98%), PGE_2-d_4 (≥99% deuterated forms (d_1-d_4)), DHA (≥98%), and DHA-d_5 (≥99% deuterated forms (d_1-d_5)) were purchased from Cayman Chemical (supplied by Sanbio B.V., Uden, The Netherlands). Isobutyl chloroformate (≥98%) was purchased at Fisher Scientific (Landsmeer, The Netherlands). Absolute ethanol (EtOH) (for analysis, EMSURE®), ethanolamine (≥99%), triethylamine (≥99.5%), Lipopolysaccharides from *Escherichia coli* O111:B4 (L3024), and Triton X-100 were purchased from Sigma Aldrich (Zwijndrecht, The Netherlands). Chloroform-*d* (100.0 atom% D) was obtained from Janssen Chimica (Beerse, Belgium). Dichloromethane (DCM) for the synthetic procedure of the standards was purified using a Pure Solv 400 solvent purification system from Innovative Technology (Amesburry, USA). Acetonitrile (ACN) (≥99.9%, HiPerSolv CHROMANORM® for LC-MS) was obtained from VWR Chemicals (Amsterdam, The Netherlands). Formic acid (FA) (99%, ULC/MS) was purchased from Biosolve B.V. (Valkenswaard, The Netherlands). Ultrapure water was filtered by a MilliQ integral 3 system from Millipore (Molsheim, France). 1× PBS (pH 7.4), Dulbecco's Modified Eagle's Medium (DMEM) and penicillin and streptomycin were purchased from Corning (supplied by Fisher Scientific, Landsmeer, The Netherlands). Fetal calf serum (FCS) was obtained from Biowest (supplied by VWR International B.V., Amsterdam, The Netherlands), Probumin® BSA was purchased from Merck (Zwijndrecht, The Netherlands).

2.2. Methods

2.2.1. Synthesis of 13-HDHEA or 16-HDHEA

Synthesis of 13-HDHEA and 16-HDHEA was performed according to a previously reported method [38]. In short, 500 μg of 13-HDHA or 16-HDHA dissolved in EtOH (1 eq., 1.45 μmol) was evaporated to dryness using co-evaporation with DCM, and dissolved in 2 mL dry DCM under argon atmosphere. Then 100 μL of a freshly prepared solution of 282 μL distilled triethylamine in 10 mL dry DCM was added (14 eq., 20.3 μmol), followed by the addition of 100 μL of a freshly prepared solution of 226

μL isobutyl chloroformate in 10 mL dry DCM (12 eq., 17.4 μmol). The solutions were stirred at room temperature for 1 h under argon atmosphere to form the mixed anhydrides, before the reaction was cooled on ice. To the mixed anhydrides 100 μL of a freshly prepared solution of 223 μL distilled triethylamine (11 eq., 16.0 μmol) and 96 μL ethanolamine (11 eq., 16.0 μmol) in 10 mL dry DCM was added. The reactions were stirred on ice for overnight. The next day the reaction mixtures were evaporated and dissolved in 500 μL water:ACN (30:70) to purify the product by preparative high pressure liquid chromatography (HPLC) (*vide infra*). After purification, 169 μg of 13-HDHEA and 151 μg of 16-HDHEA were obtained, which equals a synthetic yield of 30% and 27%, respectively. NMR spectra and LC-HRMS chromatograms of the obtained compounds are provided in the Supplementary information (Figs. S1–S18).

2.2.2. Preparative HPLC

13-HDHEA and 16-HDHEA were purified on a Zorbax Eclipse XDB-C18 column (9.4 × 250 mm, 5 μ) from Agilent Technologies B.V. (Amstelveen, The Netherlands). The purification was performed using an isocratic run of 30:70 water:ACN containing 0.1% FA with a flow rate of 4 mL/min. The purified compounds were evaporated to dryness using a rotary evaporator and subsequent freeze drying. The samples were dissolved in absolute EtOH for quantification and use in cell culture experiments.

2.2.3. HPLC quantification

Subsequent quantification of the HDHEA compounds was based on the UV absorption at 240 nm, caused by the conjugated diene structure in the oxidized PUFAs and their ethanolamine derived product; the UV-absorption of DHEA indicated that the amide structure of the endocannabinoid does not contribute to the 240 nm absorption (Figs. S19–S27). Calibration curves of 13-HDHA and 16-HDHA were injected in concentrations ranging from 0 to 100 μg/mL in duplicate, using 10 μL per injection (Figs. S28–S29). The chromatography was performed on a Zorbax Eclipse XDB-C18 column (4.6 × 250 mm, 5 μ) from Agilent Technologies B.V. (Amstelveen, The Netherlands), using an isocratic run of 30:70 water:ACN containing 0.1% FA with a flow rate of 1 mL/min.

2.2.4. Cell incubations

RAW264.7 macrophages (American Type Culture Collection, Teddington, UK) were cultured in DMEM containing 10% fetal calf serum (FCS) and 1% penicillin and streptomycin (P/S) at 37 °C in a 5% CO_2 humidified incubator. For the incubations 2 mL of 250.000 cells/mL were seeded in 6-wells plates. After 24 h, the medium of the adherent cells was discarded and replaced by fresh medium containing vehicle (0.1% EtOH), DHEA, 13-HDHEA, 16-HDHEA or a combination of 13-HDHEA and 16-HDHEA. During the incubations, the final concentration of EtOH was preserved at 0.1% in DMEM. After 30 min. pre-incubation with the compounds, the macrophages were stimulated with 1.0 μg/mL LPS. This was achieved by adding 20 μL of 100 μg/mL LPS (10% PBS in medium) to the cells. Control incubations without LPS were supplied with 20 μL 10% PBS in medium. After 24 h, the medium of the adherent cells was used for biological assays immediately or stored at −80 °C. The cells were lysed using RLT buffer from Qiagen Benelux B. V. (Venlo, The Netherlands) to extract the RNA from the macrophages (*vide infra*), which was stored at −80 °C. Experiments were performed three times using technical duplicates.

2.2.5. Cell cytotoxicity

To evaluate the cytotoxicity of the added compounds an LDH cytotoxicity Kit form Roche (Woerden, The Netherlands) was used to measure extracellular lactate dehydrogenase. The LDH assay was measured immediately after collection of the sample medium. In short, 50 μL of a reagent solution (1:45 LDH reagent 1:LDH reagent 2) was mixed with 50 μL of sample medium. The plate was then incubated at room temperature until the positive control (cells treated with 1% Triton X-100) colored dark red. The reaction was quenched with 25 μL of 1.0 M HCl before the absorbance was read with a plate reader at 492 nm.

2.2.6. Determination of NO concentration

The NO production in LPS stimulated macrophages was measured using a Griess assay from Cayman Chemical (supplied by Sanbio B.V., Uden, The Netherlands). The Griess assay was performed directly after collection of the medium. The assay was performed by adding 50 μL of Griess Reagent 1 and 50 μL Griess Reagent 2 to 100 μL of the medium. The samples were mixed at room temperature until the colour developed. The samples were compared to a nitrite standard ranging from 0 to 35 μM, after blank subtraction. The samples were measured on an ELISA plate reader at 540 nm.

2.2.7. Determination of cytokine concentrations

Concentrations of excreted IL-6, IL-1β, IL-1Ra, and TNFα in the sample medium of the 24 h treated macrophages were determined by the appropriate ELISA assays [*i.e.* a mouse IL-6 DuoSet ELISA, mouse IL-1ra/IL-1F3 DuoSet ELISA, mouse IL-1 beta/IL-1F2 DuoSet ELISA, and mouse TNF-alpha DuoSet ELISA were purchased from R&D systems (Abingdon, UK)] according to manufacturer's descriptions. IL-1β concentration was determined in undiluted medium samples; IL-1Ra was determined in 10× diluted medium samples; TNFα and IL-6 concentrations were determined in 100× diluted medium samples.

2.2.8. Transcriptome analysis

Cellular incubations with the compounds were performed three times containing technical duplicates. RNA from the technical duplicates were pooled for each separate experiment, thereby obtaining a single RNA sample from each condition for each of the three independent experiments. For the transcriptome analyses we used RNA from vehicle (0.1% EtOH), 5.0 μM 13-HDHEA, 5.0 μM 16-HDHEA, or 2.5 μM 13-HDHEA plus 2.5 μM 16-HDHEA incubated 1.0 μg/mL LPS stimulated RAW264.7 macrophages. Macrophages were stimulated with 1.0 μg/mL LPS 30 min. after pre-incubation with the compounds or vehicle.

RNA from the lysed macrophages was purified according to the manufacturers' description using a RNeasy© Micro kit from Qiagen Benelux B.V. (Venlo, The Netherlands). After purification on the columns, the RNA was eluted using 20 μL of RNAse free water. RNA concentration was determined using nanodrop, and RNA quality was assessed using RNA 6000 nanochips on the Agilent 2100 bioanalyzer from Agilent Technologies B.V (Amstelveen, the Netherlands). All RNA exceeded a RNA integrity number (RIN) of 9.5. Per sample, 100 ng of purified total RNA was labeled with the Whole-Transcript Sense Target Assay kit from Affymetrix (Life Technologies, Bleiswijk, The Netherlands, P/N 902281), which was hybridized to an Affymetrix GeneChip Mouse Gene 2.1 ST arrays (Life Technologies, Bleiswijk, The Netherlands). Hybridization, washing, and scanning of the peg arrays were carried out on an Affymetrix GeneTitan instrument according to the recommendations of the manufacturer.

Microarray quality control and data analysis pipeline have been described in detail previously [39]. Briefly, normalized expression estimates of probe sets were computed by the robust multiarray analysis (RMA) algorithm [40] as implemented in the Bioconductor library *oligo* [41]. Probe sets were redefined using current genome information according to Dai et al. [42] based on annotations provided by the Entrez Gene database, which resulted in the profiling of 27,381 unique genes (custom CDF v24). Differentially expressed probe sets (genes) compared to the vehicle control were identified by using linear models (library *limma*) and an intensity-based moderated t-statistic [43–45]. The heterogeneity in gene expression profiles that was observed in PCA plots was taken into account by fitting a heteroskedastic model that included relative quality weights that were computed for each sample per experimental group [46,47]. Probe sets that satisfied the criterion of moderated P-value <0.01, and average gene expressions (average log2 expression >3.5) were considered to be significantly regulated (Table

S1).

The microarray data set has been submitted to the Gene Expression Omnibus (accession number GSE160086).

2.2.9. IPA analysis

Functional and Upstream Regulator analysis was performed using Ingenuity Pathway Analysis (IPA®) (http://www.ingenuity.com/science/knowledgebase) from Qiagen Benelux B.V. (Venlo, The Netherlands) in July 2020. The Ingenuity Knowledge Base is a knowledge repository that houses the biological and chemical relationships extracted from the scientific literature, and this information was used to analyze the effects between transcriptional regulators (from transcription factor, to microRNA, kinase, compound or drug, that affects the expression of other molecules) and their target genes. IPA® examines how many known gene targets of each transcription regulator are present in the data set, and compares both direction and change (expression of the gene in the 13- and 16-HDHEA treatment compared to the vehicle) to stored pathways extracted from literature (http://pages.ingenuity.com/IngenuityUpstreamRegulatorAnalysisWhitepaper.html). Using this prediction tool, potential upstream regulators and potential cellular processes that may have been affected by 13- and 16-HDHEA are identified.

Differentially expressed genes between vehicle treated LPS stimulated macrophages and the HDHEA (5.0 μM 13-HDHEA, 5.0 μM 16-HDHEA, 2.5 μM 13-HDHEA and 2.5 μM 16-HDHEA combined) treated LPS-stimulated macrophages were included in the input of the IPA® analysis. In the output the upstream transcriptional regulators were scored using an activation Z-score. Cut-off values for the activation Z-score are 2.0 for induced upstream regulators or −2.0 for inhibited upstream regulators. Similarly, Z-score cut-offs of 2.0 and −2.0 were used in diseases and functions analysis. Moderated P values give significance of the observed regulator pathways and functions. In the results only significant ($P < 0.01$) pathways and functions are displayed.

2.2.10. LC-MS/MS quantification of oxylipins and PUFAs

LC-MS/MS-based quantification of various eicosanoids and PUFAs was performed by extracting 187.5 μL sample medium with 1.5 mL MeOH containing 1.33 ng/mL of the internal standards PGE_2-d_4, 5-HETE-d_8, LTD_4-d_5, DHA-d_5 on ice for 30 min. The samples were centrifuged at 4 °C at 14000 rpm, after which the supernatant was diluted with 6 mL ultrapure water containing 0.1% formic acid (FA). The samples were purified over HLB oasis SPE columns from Waters Chromatography B.V. (Breda, The Netherlands). The columns were activated using 2 mL of MeOH, and equilibrated using 2 mL ultrapure water containing 0.1% FA. Subsequently the samples were loaded, after which the columns were washed using 2 mL 20% MeOH in ultrapure water containing 0.1% FA. The columns were dried for 15 min. and the oxylipins and PUFAs were eluted using 1 mL MeOH. The eluates were collected in borosilicate glass vials containing 20 μL of 500 μM butylated hydroxytoluene and 10% glycerol in EtOH to prevent oxidation of the oxylipins and to allow for proper evaporation on a Turbovap evaporator (Biotage; Uppsala, Sweden). The samples were dissolved in 100 μL of absolute EtOH, after which 6 μL of the samples were injected on an ultra-high pressure liquid chromatography (UPLC) coupled to a TQS mass spectrometer from Waters Chromatography B.V. (Breda, The Netherlands). The MS settings were optimized and measured in the negative ionization mode using 2.5 kV capillary voltage, 40 V cone voltage, source offset 20, 600 °C desolvation temperature. The chromatographic separation was accomplished on a Zorbax Eclipse Plus C18 column 2.1 × 150 mm, 1.8 μ from Agilent Technologies B.V. (Amstelveen, The Netherlands) using gradient elution with solvent A containing 5% ACN in ultrapure water with 0.1% FA, and solvent B containing 100% ACN with 0.1% FA. The gradient started by applying 5% B in A followed by a linear increase to 30% B, which was achieved at 5 min. This was followed by a linear increase towards 50% B, which was achieved at 11.25 min. and maintained until 13.25 min. The system was subsequently switched to 100% B which was achieved at 15.75 min. and maintained until 18.75 min., after which the system was equilibrated at 5% B until 22 min. The mass fragmentation settings were optimized per compound (Table S2). Peak identification and quantification were performed using TargetLynx version 4.1 software from Waters Chromatography B.V. (Breda, The Netherlands). Quality control samples were included to check the quality of the analysis.

2.2.11. Statistical analyses

Experiments were performed three times containing two technical replicates. Data is expressed as average percentage relative to 1.0 μg/mL LPS treated vehicle control (set as 100%) containing standard deviation or standard error of the mean. Statistical analysis was performed using a non-parametric one-way ANOVA followed by a Dunnet's *t*-test. P-values assigned as statistically relevant are classified as $P < 0.05$, $P < 0.01$, $P < 0.001$. Statistical differences between treatments were shown if an effect was found on 13- and 16-HDHEA (non-parametric one-way ANOVA followed by a Tukey multiple comparison test, *post hoc*).

3. Results

3.1. Cytotoxicity of test compounds

Cytotoxicity of DHEA, 13-HDHEA and 16-HDHEA was evaluated by measuring the LDH release from 1.0 μg/mL LPS-stimulated and incubated RAW264.7 macrophages. Macrophages were incubated for 24.5 h with 2.5 μM and 5.0 μM of the test compounds, or a combination of 2.5 μM 13-HDHEA and 2.5 μM 16-HDHEA. Neither the individual compounds nor the combination showed a significant cytotoxic effect on the macrophages when compared to the vehicle control with 1.0 μg/mL LPS stimulation (Fig. S30).

3.2. 13- and 16-HDHEA do not reduce LPS induced NO and IL-6 release

The effects of 13- and 16-HDHEA and DHEA on the release of the inflammatory mediators NO and IL-6 were investigated using LPS-stimulated RAW264.7 macrophages. No significant effect was observed for 13-HDHEA and 16-HDHEA on NO release after 24.5 h, whereas the parent compound DHEA caused a small but significant inhibition for NO (Fig. 2a). Statistical testing showed that DHEA treatment significantly reduced NO release (71 ± 6% at 2.5 μM DHEA ($P < 0.05$); 66 ± 18% at 5 μM DHEA ($P < 0.05$)).

Similarly, 13-HDHEA and 16-HDHEA did not affect IL-6 production (Fig. 2b). DHEA again showed a significant reduction of IL-6 production (75 ± 6% at 2.5 μM DHEA ($P < 0.01$); 77 ± 11% at 5 μM DHEA ($P < 0.05$)).

3.3. 13-HDHEA reduces LPS induced production of TNFα and IL-1β

Incubation of LPS-stimulated cells with 5 μM 13-HDHEA resulted in lower TNFα concentrations (83 ± 7% ($P < 0.05$)) compared to the vehicle (Fig. 2c). Incubations with DHEA also caused significant reduction of TNFα production (82 ± 4% at 2.5 μM DHEA ($P < 0.001$); 88 ± 2% at 5 μM DHEA ($P < 0.01$)). Statistical analysis using Tukey's multiple comparison test showed no additional significant differences between the various treatments.

Incubation of LPS-stimulated cells with 5 μM 13-HDHEA also significantly reduced IL-1β cytokine concentrations (78 ± 6% ($P < 0.05$)) compared to the vehicle (Fig. 2d). In addition, IL-1β concentration was reduced by the combined incubation with 2.5 μM 13-HDHEA and 2.5 μM 16-HDHEA (80 ± 8% ($P < 0.05$)). DHEA also reduced IL-1β cytokine levels (71 ± 2% at 2.5 μM DHEA ($P < 0.001$); 59 ± 9% at 5 μM DHEA ($P < 0.001$)). Statistical analysis using Tukey's multiple comparison test indicated that 5 μM DHEA treatment was significantly more effective in reducing IL-1β compared to 2.5 μM 13-HDHEA and 16-HDHEA ($P < 0.05$), but not compared to 5 μM 13-HDHEA.

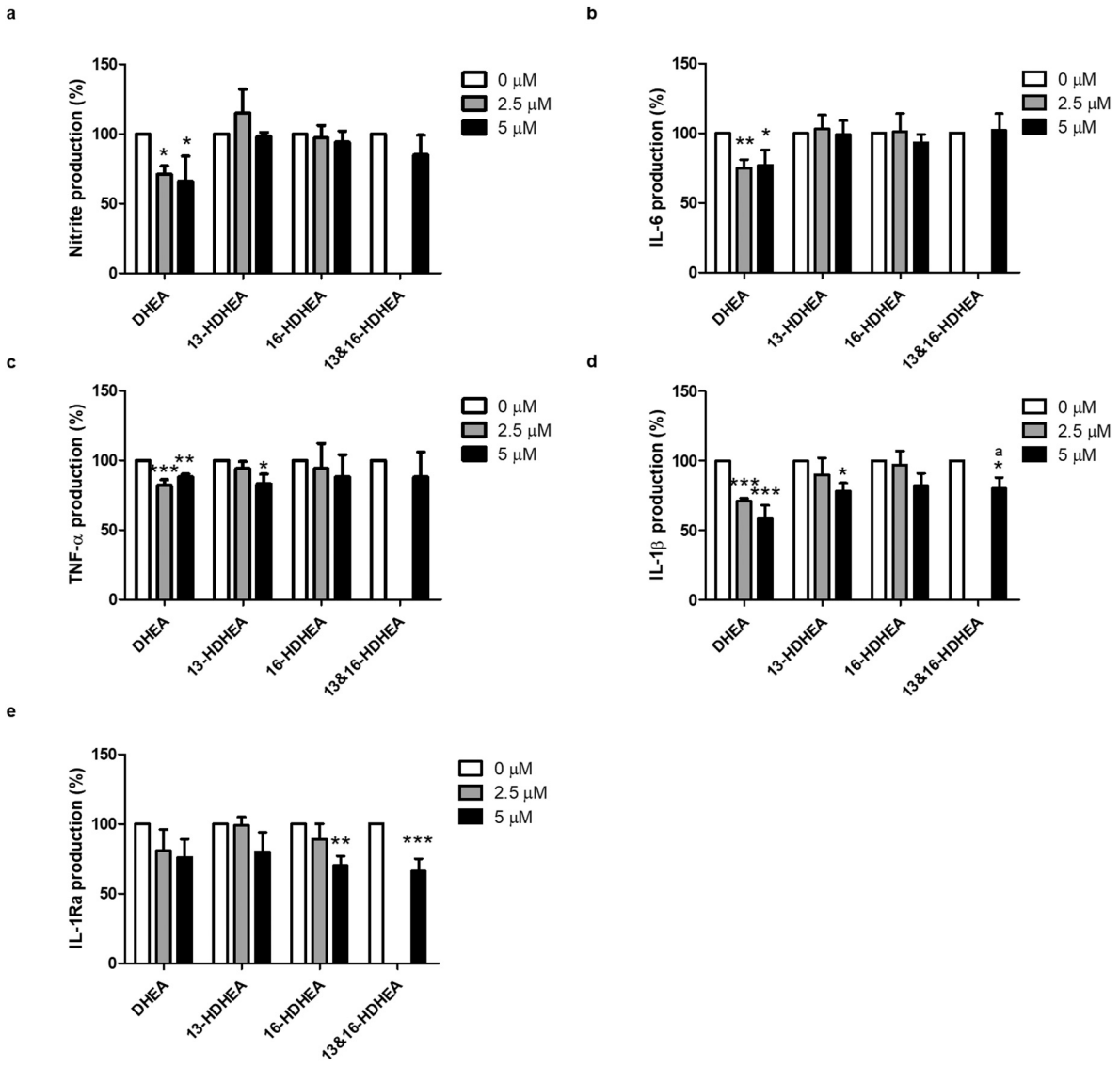

Fig. 2. Production of NO (a), IL-6 (b), TNFα (c), IL-1β (d), and IL-1Ra (e) released from 1.0 μg/mL LPS stimulated RAW264.7 macrophages, incubated with 2.5 μM or 5 μM DHEA, 13-HDHEA, 16-HDHEA and a combined exposure to 2.5 μM 13-HDHEA and 2.5 μM 16-HDHEA. Cells were pre-treated with the compounds for 30 min. before 1.0 μg/mL LPS addition and incubation of 24 h. Data are expressed as % relative to the vehicle control with 1.0 μg/mL LPS (=100%). Bars represent averages with SD from n = 3 independent experiments containing technical duplicates. Asterisks indicate significant differences from the vehicle with 1.0 μg/mL LPS control (one-way ANOVA, Dunnett's *t*-test *post hoc*; * $P < 0.05$, ** $P < 0.01$, *** $P < 0.001$). Statistical testing showed significant effects compared to 5 μM DHEA treatment (a) (one-way ANOVA, Tukey multiple comparison test *post hoc*; $P < 0.05$).

3.4. 13- and 16-HDHEA reduce LPS induced production of IL-1Ra

Incubation of LPS-stimulated cells with 13-HDHEA and 16-HDHEA displayed inhibiting trends on IL-1Ra production (Fig. 2e). The combined incubation with 2.5 μM 13-HDHEA and 2.5 μM 16-HDHEA (66 ± 9% ($P < 0.001$)), and the incubation with only 5 μM 16-HDHEA (70 ± 7% ($P < 0.01$)) reduced IL-1Ra productions. Incubations with only 13-HDHEA or DHEA did not result in a significant reduction of IL-1Ra. Statistical analysis using Tukey's multiple comparison test showed no additional significant differences between the various tests.

3.5. 13- and 16-HDHEA reduce expression of InhbA and Ifit1, and induce expression of SerpinB2, Ptgsh1, Alox5 and Ppbp

Because 13-HDHEA and 16-HDHEA showed relatively moderate immunomodulating effects on the production and release of inflammatory mediators NO, IL-6, IL-1Ra, IL-1β, and TNF-α in LPS-stimulated macrophages, it was decided to continue exploring the effects of 13- and 16-HDHEA by investigating the effects on the full gene expression profile of LPS-stimulated RAW264.7 macrophages. For transcriptome analysis, incubations with 5 μM 13-HDHEA, 5 μM 16-HDHEA, and the combination of 2.5 μM 13-HDHEA and 2.5 μM 16-HDHEA were compared to the vehicle control. Transcriptome analysis revealed 203 differentially expressed genes for exposure to 13-HDHEA, 120 differentially expressed genes for incubation with 16-HDHEA, and 165 differentially expressed genes for the combined 13-HDHEA and 16-HDHEA exposure (Table S1). For 13-HDHEA exposure the ribosomal protein L23A (Rpl23a) gene was most strongly induced, and the predicted gene 15754 (Gm15754) was most strongly reduced. For 16-HDHEA strongest induction was obtained for melanoma antigen, family A, 2 (Magea2), and highest reduction was obtained for gasdermin C-like 2 (Gsdmcl2). Combined incubation with 13-and 16-HDHEA resulted in strongest induction of the predicted gene 7665 (Gm7665), and highest reduction of an unannotated gene. Twenty of the differentially expressed genes were shared among the various incubations with HDHEA (Fig. 3, Table 1). Among these genes, pro-platelet basic protein

(Ppbp) was most strongly induced by 13-HDHEA, whereas GM4924 was most strongly induced by 16-HDHEA. Interestingly, the inflammatory resolution related gene serine peptidase inhibitor, clade B, member 2 (SerpinB2) was significantly induced by HDHEA exposure [48]. Next to the induction of resolution related genes, inhibition of the inflammatory regulating genes interferon-induced protein with tetratricopeptide repeats 1 (Ifit1) and inhibin beta-A (InhbA) was observed [49,50]. Finally, the oxylipin regulating genes prostaglandin-endoperoxide synthase 1 (Ptgsh1) and arachidonate 5-lipoxygenase (Alox5) were also found to be induced in all conditions tested.

3.6. Upstream regulator pathway analysis reveals an anti-inflammatory signature for 13- and 16-HDHEA

In order to investigate whether the observed changes in gene expression show a consistent pattern or relation with known regulators and pathways, Ingenuity Pathway Analysis (IPA®) was performed (*July 2020*). Identified upstream regulators show that an anti-inflammatory signature is apparent (Fig. 4). Many of the upstream regulators were classified by IPA® as potentially inhibited, like TLR4, MyD88, IRF3, IRF7, STAT1, and several IFNs are involved in LPS signaling through TLR4 [51,52]. Potentially induced regulators like IL-10RA, SIRT-1, and that of the anti-inflammatory drug fluticasone propionate are generally involved in anti-inflammatory processes [53–55]. Analysis of stimulated macrophages incubated with 16-HDHEA at 5 μM did not reveal any significantly affected upstream regulators.

Functional IPA® analysis was performed in order to link the alterations in expression to physiological processes with similar changes. This approach generates hypotheses concerning the functional consequences of the observed changes in gene expression. The functional IPA® analyses suggested that 5 μM 13-HDHEA changed the expression of gene sets associated with a decrease in angiogenesis, apoptosis of prostate cancer cells, and the development of epithelial tissue (Fig. 5a).

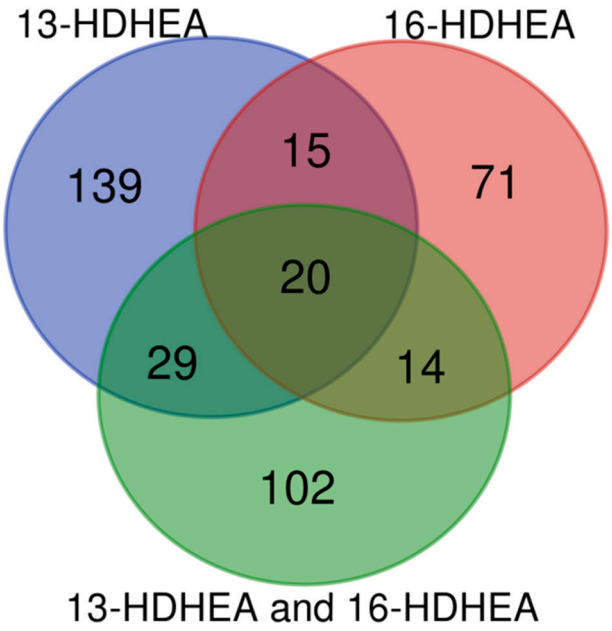

Fig. 3. Venn diagram showing overlap of significantly expressed genes ($P < 0.01$ and average log2 expression value >3.5) of the 1.0 μg/mL LPS stimulated RAW264.7 macrophages, incubated with 5 μM 13-HDHEA (blue), 5 μM 16-HDHEA (red), and a combinatorial 2.5 μM 13-HDHEA and 2.5 μM 16-HDHEA incubation (green). Cells were incubated for 24 h, and pre-treated with the compounds 30 min. before LPS addition. Experiments were performed three times individually with pooled technical duplicates. The Venn diagram was drawn using the free online Venn diagram drawing tool (http://bioinformatics.psb.ugent.be/webtools/Venn/).

Subsequently, gene sets associated with cell movement, adhesion of immune cells, degeneration of connective tissue, and production of radical oxygen species (ROS) for 5 μM 13-HDHEA were identified as potentially induced (Fig. 5b). Incubation with 5 μM 16-HDHEA also resulted in regulation of gene sets associated with an increase in cell movement of phagocytes and adhesion of immune cells (Fig. 5c). The combined incubation with 2.5 μM 13-HDHEA and 2.5 μM 16-HDHEA only pointed to potential increased inflammatory functions (Fig. 5d).

3.7. 13- and 16-HDHEA do not affect oxylipin profiles

Giving the inducing effects of 13-HDHEA and 16-HDHEA on the expression of the lipid metabolizing genes Ptgs1, Alox5 (Table 1), and the inducing effect of 13-HDHEA on leukotriene synthase C4 (Ltc4s) (Table S1), we continued with lipidomic analyses to further validate the consequences of the altered gene expression levels of these lipoxygenases. To this end, a targeted LC-MS/MS method was developed to detect 5-HETE and LTB_4 as Alox5 products, LTC_4 and LTD_4 as products of Ltsc4, PGE_2 and PGD_2 as Ptgsh1 (also known as COX-1) and Ptgsh2 (also known as COX-2) products, and DHA as DHEA precursor in LPS-stimulated macrophages. PGE_2 excretion was significantly inhibited by DHEA (38 ± 6% at 2.5 μM ($P < 0.001$); 21 ± 10% at 5 μM DHEA ($P < 0.001$)) (Fig. 6a). With 13-HDHEA and 16-HDHEA exposed cells no significant inhibition of the LPS induced PGE_2 production was obtained. Similarly, PGD_2 excretion was significantly reduced DHEA (40 ± 6% at 2.5 μM ($P < 0.001$); and 26 ± 10% at 5 μM DHEA ($P < 0.001$)) (Fig. 6b), and both 13-HDHEA and 16-HDHEA did not cause a reduction of PGD_2 production. For the combination of 2.5 μM 13- and 16-HDHEA even a small but significant induction of PGD_2 production was obtained. DHA levels were found to be significantly decreased by 13-HDHEA (69 ± 26% at 2.5 μM ($P < 0.05$); 70 ± 14% at 5 μM ($P < 0.05$)), by 5 μM 16-HDHEA (64 ± 34% ($P < 0.05$)), and by the combination of 2.5 μM 13- and 16-HDHEA (73 ± 32% ($P < 0.05$)). In contrast to a reduction of DHA formation after incubation with HDHEA, DHEA seemed to give an increasing trend on the DHA levels (Fig. 6c). Statistical testing using a one-way ANOVA multiple comparisons test using Tukey's statistics indicated a significant difference in DHA levels between 5 μM DHEA and 5 μM 16-HDHEA ($P < 0.001$), 5 μM 13-HDHEA ($P < 0.01$), and the combination of 2.5 μM 13-HDHEA and 16-HDHEA ($P < 0.01$). Levels of 5-HETE, LTB_4, LTC_4, and LTD_4 could not be quantified, because the concentrations were below the LOD.

4. Discussion

In this study we explored the biological effects of the recently discovered DHEA metabolites 13- and 16-HDHEA in LPS-stimulated RAW264.7 macrophages [38]. Potential immunomodulating effects of 13- and 16-HDHEA were studied on cytokine release, transcriptome analysis, and *via* the production of several oxylipin mediators. In short, 13-HDHEA at medium concentrations of 5 μM significantly reduced production of TNF-α and IL-1β in LPS-stimulated macrophages, and incubation with 5 μM 16-HDHEA led to a significant reduction of IL-1Ra production. The combination of 2.5 μM 13-HDHEA and 2.5 μM 16-HDHEA in the medium led to a significant decrease in IL-1β and IL-1Ra production. In contrast to the parent DHEA, 13- and 16-HDHEA did not reduce LPS-induced IL-6 and NO levels. Transcriptome analysis revealed an anti-inflammatory signature for both 13-HDHEA and 16-HDHEA. Incubation with 13-HDHEA and 16-HDHEA induced the resolution related gene SerpinB2, and was predicted to induce anti-inflammatory regulated pathways, including IL-10, Sirt-1, and those mimicking anti-inflammatory effects of the corticosteroid fluticasone propionate. Additionally, 13-HDHEA and 16-HDHEA inhibited inflammatory regulating genes Ifit1 and InhbA, and were predicted to deactivate several downstream regulators of LPS activation. Finally, targeted lipidomic analysis revealed that in contrast to DHEA, 13- and 16-HDHEA do not reduce PGE_2 and PGD_2 production after LPS stimulation, but led

Table 1
Fold change of significantly induced and reduced genes (P < 0.01) between the vehicle exposed LPS stimulated RAW264.7 macrophages and the 5 μM 13-HDHEA, 5 μM 16-HDHEA, and 2.5 μM combinatorial 13-HDHEA and 16-HDHEA exposed LPS-stimulated macrophages after 24 h incubation. Only genes with an average log2 expression value >3.5 (Average Expr >11.314) are listed. Genes inhibited by the incubation of our compounds are displayed in green, genes induced by exposure to the compounds are displayed in red. LPS stimulation was performed using 1.0 μg/mL LPS 30 min. after pre-treatment of the compounds. Data obtained from three independent experiments with pooled technical duplicate incubations.

Gene Symbol	13-HDHEA vs Vehicle	16-HDHEA vs Vehicle	13&16-HDHEA vs Vehicle	Average Expr	Gene Name
Plin2	1.285	1.179	1.242	1796.082	perilipin 2
1110008P14Rik	1.140	1.174	1.138	955.671	RIKEN cDNA 1110008P14 gene
Csf2rb	1.237	1.254	1.243	768.796	colony stimulating factor 2 receptor, beta, low-affinity (granulocyte-macrophage)
Pf4	1.188	1.216	1.187	775.378	platelet factor 4
Smox	1.259	1.242	1.236	452.344	spermine oxidase
Serpinb2	1.276	1.346	1.333	287.437	serine (or cysteine) peptidase inhibitor, clade B, member 2
Lsm3	1.261	1.210	1.224	201.941	LSM3 homolog, U6 small nuclear RNA and mRNA degradation associated
Fcgr3	1.315	1.272	1.269	155.375	Fc receptor, IgG, low affinity III
C130050O18Rik	1.479	1.247	1.239	150.907	RIKEN cDNA C130050O18 gene
Ptgs1	1.314	1.246	1.289	104.593	prostaglandin-endoperoxide synthase 1
Frmd6	1.267	1.295	1.337	90.337	FERM domain containing 6
Alox5	1.416	1.302	1.425	76.133	arachidonate 5-lipoxygenase
Mir466f-4	1.320	1.344	1.274	86.522	microRNA 466f-4
Mir3075	1.694	1.605	1.551	27.848	microRNA 3075
Gm4924	1.475	1.716	1.515	13.016	predicted gene 4924
Ppbp	2.069	1.399	1.621	12.278	pro-platelet basic protein
Selenos	-1.149	-1.143	-1.155	412.811	selenoprotein S
Ifit1	-1.358	-1.215	-1.346	376.919	interferon-induced protein with tetratricopeptide repeats 1
Clcn7	-1.157	-1.166	-1.210	375.762	chloride channel, voltage-sensitive 7
Inhba	-1.353	-1.314	-1.428	86.121	inhibin beta-A

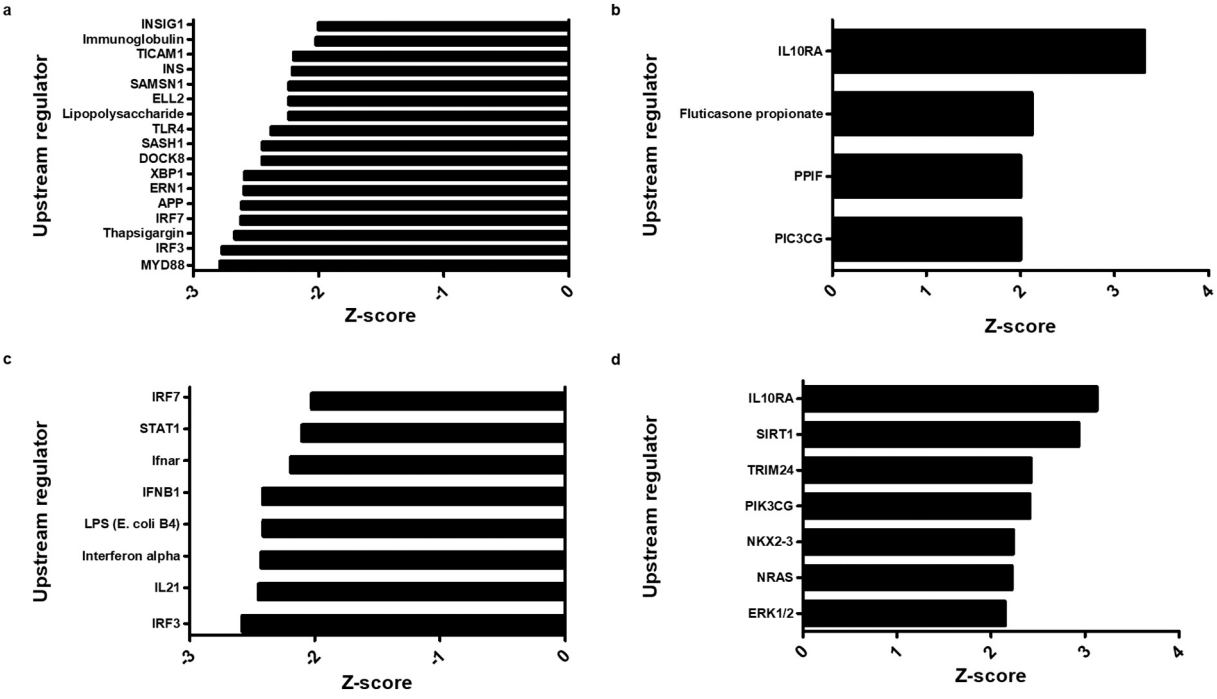

Fig. 4. Activation Z-scores of affected upstream regulators of 5 μM 13-HDHEA treated (a and b) and 2.5 μM 13-HDHEA and 2.5 μM 16-HDHEA combined treatment (c and d) in 1.0 μg/mL LPS stimulated RAW264.7 macrophages. Upstream regulators shown have a Z-score < −2.0 (A and C) or Z-score > 2.0 (b and d), and are significant compared to the vehicle control (P < 0.01).

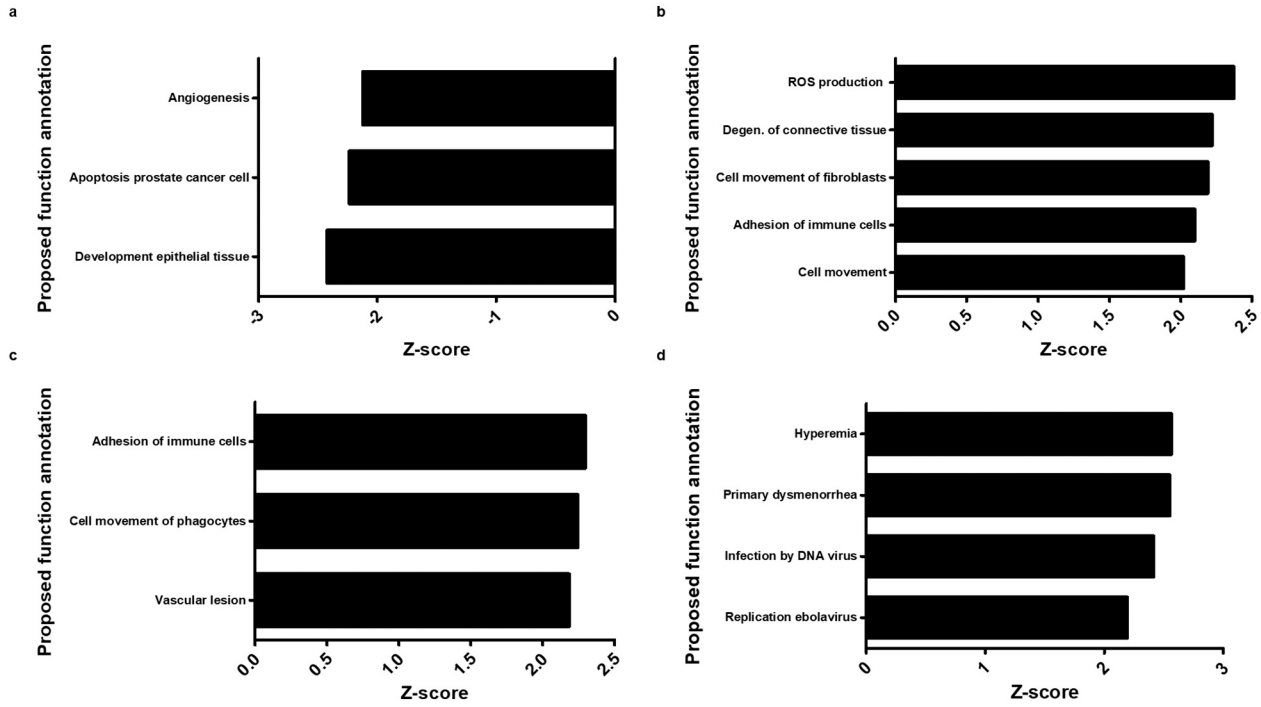

Fig. 5. Activation Z-scores of disease and function annotations of 5 μM 13-HDHEA treated (a and b), 5 μM 16-HDHEA (c), and 2.5 μM 13-HDHEA and 2.5 μM 16-HDHEA combined treatment (d) of 1.0 μg/mL LPS stimulated RAW264.7 macrophages. Inhibited diseases and functions have a Z-score < -2.0 (a), and induced diseases and functions have a Z-score > 2.0 (b–d). All diseases and functions are significantly affected compared to the vehicle control ($P < 0.01$).

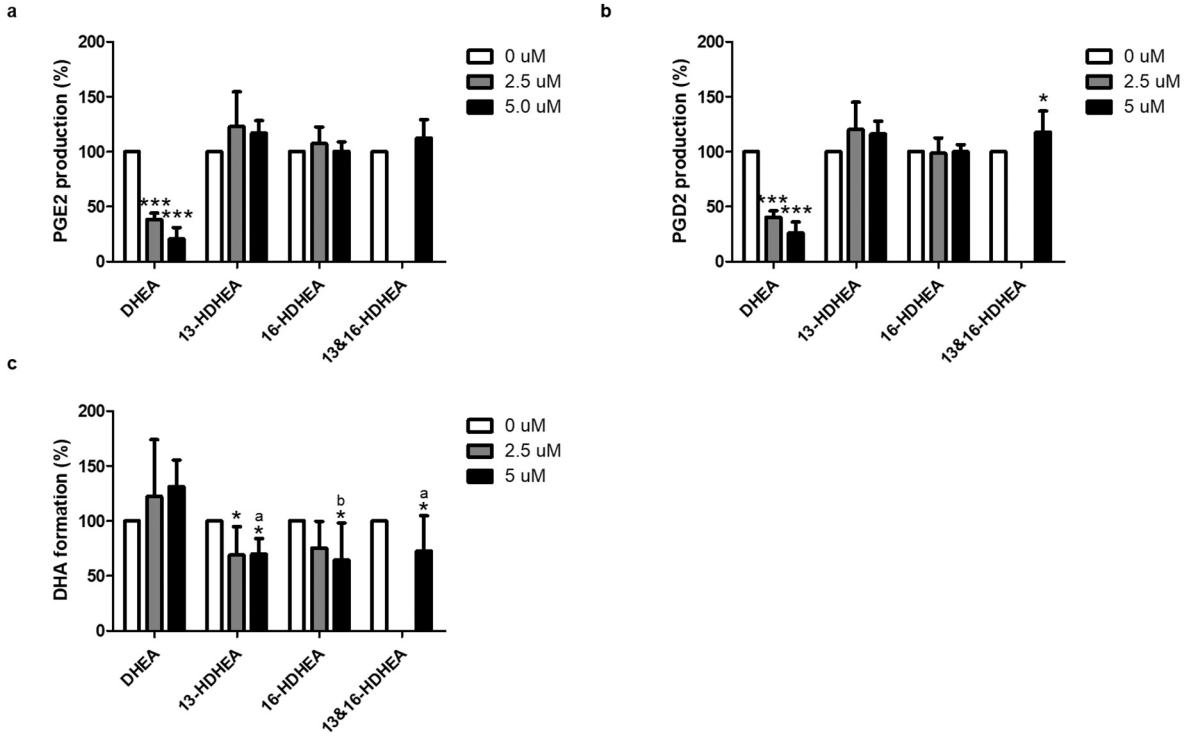

Fig. 6. Release of PGE_2 (a), PGD_2 (b), and DHA (c) from 1.0 μg/mL LPS stimulated RAW264.7 macrophages, incubated with 2.5 μM or 5 μM DHEA, 13-HDHEA, 16-HDHEA, and a combined treatment of 2.5 μM 13-HDHEA and 2.5 μM 16-HDHEA as determined by LC-MS/MS. Cells were pre-treated with the compounds for 30 min. before 1.0 μg/mL LPS addition and incubation of 24 h. Data are expressed as % relative to the vehicle and 1.0 μg/mL LPS treated control (=100%). Bars represent means with SD from $n = 3$ independent experiments containing technical duplicates. Asterisks indicate significant differences from the vehicle control (one-way ANOVA, Dunnett's *t*-test *post hoc*; * $P < 0.05$, *** $P < 0.001$). Statistical testing showed significant effects compared to 5 μM DHEA treatment $P < 0.01$ (a) or $P < 0.001$ (b) (one-way ANOVA, Tukey multiple comparison test *post hoc*).

to a remarkable decrease of DHA in the cell medium. Even though 13- and 16-HDHEA display anti-inflammatory effects in LPS-stimulated RAW264.7 macrophages, these effects are less pronounced compared to DHEA.

The anti-inflammatory effects of 13- and 16-HDHEA stand out from other known DHEA metabolites that have been previously described in the literature. For instance, 5 μM of 19(20)-EDP-EA, a predominant metabolite produced by CYP450, showed a significant reduction in NO release and IL-6 production in 25 ng/mL LPS-stimulated BV-2 microglial cells [36]. In contrast to these observations, our model revealed that 5 μM of 13- or 16-HDHEA did not inhibit IL-6 and NO production, which might indicate a distinct anti-inflammatory profile between the CYP450- and COX-2-derived DHEA metabolites. A direct comparison can, however, not be made due to differences in the experimental setup such as a difference cell model and a substantially lower LPS concentration compared to our model. In the current study we specifically chose a relatively strong LPS stimulation of 1.0 μg/mL to maintain conditions identical to the conditions in which 13- and 16-HDHEA were formed, as well as to conditions in studies on the immuno-modulating effects of DHEA and other DHA-derived endocannabinoids that were previously performed in our laboratory [32,33,38,56,57].

Additionally, the effects of 13- and 16-HDHEA also seem to stand out from the 15-LOX products 10,17-diHDHEA and 15-HEDPEA. 10,17-diHDHEA and 15-HEDPEA were previously found to reduce platelet-leukocyte aggregation in human whole blood at concentrations as low as 10 pM, whereas DHEA showed no activity up to 100 nM. Moreover, 15-HEDPEA and 10,17-diHDHEA showed increased CB_2 receptor activation when compared to DHEA [35]. Consequently, the 15-LOX metabolites seem to have increased anti-inflammatory potential compared to DHEA, whereas 13- and 16-HDHEA generally seem to be less anti-inflammatory than DHEA. Nevertheless, due to differences in the experimental setup, a lack of DHEA control experiment in several other 15-LOX metabolite anti-inflammatory tests, differences in anti-inflammatory markers and mechanisms measured, and the use of different models, a direct and conclusive comparison between the anti-inflammatory potential of 15-LOX metabolites and 13- and 16-HDHEA cannot be made.

Transcriptome analysis was performed to investigate mechanistic immunomodulating effects of 13- and 16-HDHEA, next to the modest anti-inflammatory behavior obtained by cytokine release. Here, expression of Ifit1 and InhbA was significantly reduced by both 13- and 16-HDHEA. Ifit1 is a key regulator in downstream TLR4 mediated LPS activation [49]. InhbA leads to the production of activin A which induces early-stage activation of RAW264.7 macrophages leading to an inflammatory response [50]. Reduction of expression of these genes therefore suggests anti-inflammatory effects induced by 13-HDHEA and 16-HDHEA. In addition, Ppbp and SerpinB2 were found to be induced by both 13- and 16-HDHEA. Ppbp is a biomarker for lung cancer, and leads to induced macrophage chemotaxis [68]. SerpinB2 reduces cell migration and promotes the resolution of inflammation, thus suggesting an anti-inflammatory role for 13- and 16-HDHEA [48]. Previously, it was observed that incubation of a different DHA derived endocannabinoid, docosahexeanoyl serotonin, reduced SerpinB2 gene expression in LPS-stimulated RAW264.7 macrophages, suggesting differential effects [56]. In addition to the direct effect on these inflammatory regulating genes, several targets linked to inflammasome activation like the IL-1 pathway, MyD88, Mir3075, SerpinB2, Neat, and Cmpk2 were significantly affected in macrophages exposed to 13-HDHEA [58,59]. These observations suggest that 13- and 16-HDHEA reduce the production of inflammasome regulators. Nonetheless, RAW264.7 cells are unable to produce functional inflammasomes, because they lack the ASC adaptor protein [60], so this cannot be experimentally verified in our model. Future experiments in different models are required to establish whether 13- and 16-HDHEA do reduce functional inflammasome formation.

Inhibition of upstream regulators involved in LPS signaling was suggested for 5 μM 13-HDHEA and the combined treatment of 2.5 μM 13-HDHEA and 2.5 μM 16-HDHEA during IPA® analysis. Examples of upstream regulators suggested to be inhibited are TLR4, MyD88, IRF3, IRF7, STAT1, and LPS itself, pointing to an anti-inflammatory effect somewhere in the LPS pathway [33,52,61]. On the other hand, upstream regulators involved in anti-inflammatory responses, like IL-10, Sirt-1, and a fluticasone propionate related pathway were suggested to be induced by 13- and 16-HDHEA [53–55]. Since IPA® analysis is limited by the overlap in gene-expression profiles of connected pathways and the input of studies in the database, it cannot be excluded that 13- and 16-HDHEA can directly interact with TLR4, or adaptor molecules like MyD88 and IRF. Function annotation analysis using IPA® suggested a potential reduction in angiogenesis and an increase in ROS production for the 5 μM 13-HDHEA incubation. The proposed anti-angiogenic effect of 13-HDHEA was further supported by its reducing activity on Ang expression (Table S1), which plays an important role in the angiogenic effect of cells [62]. Moreover, SerpinB2 was found to decrease cancer metastasis and macrophage migration, which could therefore also be linked to anti-angiogenic effects [48]. Other oxidized DHEA metabolites like the CYP450-produced derivatives also demonstrated strong anti-angiogenic properties [36,37]. The proposed ROS production of 13-HDHEA was further supported by previous research showing that the interaction between DHEA and the enzymes COX-2 and 5-LOX resulted in increased ROS production in head and neck squamous cell carcinoma cells [63]. Moreover, perilipin 2 (Plin2) induction is known to increase ROS formation (Table 1) [64]. Interestingly, Plin2 is regulated via activation of CB_1, which could directly be targeted by the CYP450 metabolites of DHEA, and the 15-LOX metabolites 10,17-diHDHEA and 15-HEDPEA [35–37,65]. Based on these observations it could be speculated that 13- and 16-HDHEA reduce angiogenesis, and increase ROS formation via the interaction with CB_1, ultimately leading to an anti-tumorigenic potential.

Since transcriptomic analysis showed 13- and 16-HDHEA mediated induction on several lipoxygenase genes (like Alox5, Ptgsh1, and Ltc4s) and DHEA itself has interactions with lipoxygenases [1], we tested the formation of several oxylipins. We found no detectable amounts of leukotrienes and 5-HETE, which corresponds with previous observations in our laboratory [33]. Incubations of the macrophages with 13- and 16-HDHEA decreased DHA levels, whereas DHEA incubations resulted in DHA formation. The latter observation is most likely explained by hydrolysis of DHEA [28,66]. Reasons for the reduction of DHA levels in the 13- and 16-HDHEA incubations are unknown. Finally, PGE_2 and PGD_2 production in LPS-stimulated cells was not affected by 13- and 16-HDHEA, whereas DHEA strongly inhibits COX-2 derived prostaglandin formation [33,38]. Transcriptome analysis suggested 13- and 16-HDHEA-mediated induction of Ptgsh1, however this remains without consequences at the metabolite level. Apparently, the COX-2 upregulation by 1.0 μg/mL LPS has a stronger effect on prostaglandin formation than the observed additional induction of COX-1. Interestingly, the observations in this study support that the neutral lipid DHEA competes with arachidonic acid in the substrate binding site of COX-2, whereas its oxidized products 13-HDHEA and 16-HDHEA do not interfere with this binding [38,67].

Comparisons in the anti-inflammatory profile of 13-and 16-HDHEA with DHEA indicated that 13- and 16-HDHEA are less effective in reducing individual mediators like NO, IL-6, TNFα, and IL-1β, but also show distinct effects on *e.g.* IL-1Ra and DHA. Interestingly, transcriptome analysis from a previously performed experiment using 10 μM DHEA showed limited overlap in expression profile with 13- and 16-HDHEA (Fig. S31), further underlining a distinct anti-inflammatory profile between DHEA and its COX-2 derived metabolites [33]. Additionally, in contrast to DHEA, 13- and 16-HDHEA do not inhibit prostaglandin formation. It remains speculative to provide a meaningful interpretation for this, or to speculate whether these differences would also be apparent during *in vivo* inflammation. The modest anti-inflammatory effects of 13-HDHEA and 16-HDHEA could also suggest that 13- and 16-HDHEA are products of an DHEA-inactivation route via

COX-2 instead of specifically produced immunomodulating compounds. In addition, the metabolic fate of 13- and 16-HDHEA is unknown. Many other lipoxygenases may be present, that could further metabolize 13- and 16-HDHEA into compounds with yet unknown effects, making biological interpretation more complex [1,19,34].

Future work should focus on the hypothesized anti-angiogenic and anti-migratory properties of 13- and 16-HDHEA, which seem to be distinct for oxidized DHEA derived metabolites [35–37]. Secondly, it should be clarified whether 13- and 16-HDHEA are terminal end-products of DHEA or whether they themselves are further metabolized. A further elucidation of the metabolism and functional consequences of 13- and 16-HDHEA could explain more about the physiological relevance of DHEA and its metabolism *in vivo*. Interestingly, epoxide derived DHEA metabolites have been quantified in Sprague–Dawley rat brain, peripheral organs [36], in metastatic mice lungs [37], and 15-LOX metabolites were found in mice brain [35], demonstrating the presence of DHEA metabolism *in vivo*. Next to the quantification of DHEA derived metabolites, future studies should focus on the immunological effect of these DHEA derived metabolites *in vivo*. Recently, it was shown that 5 mg/kg i.p. injected DHEA exerts inhibitory effects on the pro-inflammatory cytokines IL-1β and TNFα in 1.0 mg/kg i.p. LPS injected mice [30]. It would be interesting to understand the potential role of the various DHEA metabolites in this and similar studies.

In conclusion, 13- and 16-HDHEA differentially inhibit LPS induced inflammation in RAW264.7 macrophages, and the observed immunomodulating effects were typically smaller and distinct from their parent compound DHEA. Future studies should elucidate whether 13- and 16-HDHEA are potential immunomodulating in different disease models (like tumorigenic and angiogenic models), and identify whether 13- and 16-HDHEA are (terminal) end-pructs of DHEA or intermediates in a further metabolization route.

Supplementary data to this article can be found online at https://doi.org/10.1016/j.bbalip.2021.158908.

CRediT authorship contribution statement

IdB, RW, BA, MBa conceived of research, wrote the manuscript, and analyzed the data. IdB performed the cell incubations, RNA isolation, and LC-MS/MS experiments. SvK and IdB measured ELISA, Griess and cytotoxicity assays, and analyzed micro-array results. GH analyzed the micro-array data and performed the statistical analysis of the micro-array data. MBo supported the IPA© analysis. MP supported in data analysis.

Declaration of competing interest

The authors declare that they have no known competing financial interests or personal relationships that could have appeared to influence the work reported in this paper.

Acknowledgements

The authors like to thank Hans Beijleveld and Frank Claassen for their assistance in the HPLC and mass spectrometry analysis of the 13-HDHEA and 16-HDHEA; Tatiana Nikolaeva and Niels de Roo for their support in NMR analysis; Fay Schrouff for her pioneering work on this project. The authors like to thank the VLAG Graduate School of Wageningen University and Research, The Netherlands for their financial support.

References

[1] I. de Bus, R. Witkamp, H. Zuilhof, B. Albada, M. Balvers, The role of n-3 PUFA-derived fatty acid derivatives and their oxygenated metabolites in the modulation of inflammation, Prostaglandins Other Lipid Mediat 144 (2019) 106351, https://doi.org/10.1016/j.prostaglandins.2019.106351.

[2] J.A. Dunstan, L.R. Mitoulas, G. Dixon, D.A. Doherty, P.E. Hartmann, K. Simmer, S. L. Prescott, The effects of fish oil supplementation in pregnancy on breast milk fatty acid composition over the course of lactation: a randomized controlled trial, Pediatr. Res. 62 (2007) 689–694, https://doi.org/10.1203/PDR.0b013e318159a93a.

[3] D. Swanson, R. Block, S.A. Mousa, Omega-3 fatty acids EPA and DHA: health benefits throughout life, Adv. Nutr. 3 (2012) 1–7, https://doi.org/10.3945/an.111.000893.

[4] L.T. Marton, R.d.A. Goulart, A.C.A.d. Carvalho, S.M. Barbalho, Omega fatty acids and inflammatory bowel diseases: an overview, Int. J. Mol. Sci., 20 (2019) 4851. doi:10.3390%2Fijms20194851.

[5] A.S. Abdelhamid, T.J. Brown, J.S. Brainard, P. Biswas, G.C. Thorpe, H.J. Moore, K. H.O. Deane, F.K. AlAbdulghafoor, C.D. Summerbell, H.V. Worthington, et al., Omega-3 fatty acids for the primary and secondary prevention of cardiovascular disease, Cochrane Database Syst. Rev. (2018), https://doi.org/10.1002/14651858.CD003177.pub3.

[6] J.E. Manson, N.R. Cook, I.M. Lee, W. Christen, S.S. Bassuk, S. Mora, H. Gibson, C. M. Albert, D. Gordon, T. Copeland, f.t.V.R.G. et al., Marine n-3 fatty acids and prevention of cardiovascular disease and cancer, New England Journal of Medicine, 380 (2018) 23–32.doi:https://doi.org/10.1056/nejmoa1811403.

[7] A. Gioxari, A.C. Kaliora, F. Marantidou, D.P. Panagiotakos, Intake of ω-3 polyunsaturated fatty acids in patients with rheumatoid arthritis: A systematic review and meta-analysis, Nutrition, 45 (2018) 114–124.e114.doi:https://doi.org/10.1016/j.nut.2017.06.023.

[8] L. Navarini, A. Afeltra, G. Gallo Afflitto, D.P.E. Margiotta, Polyunsaturated fatty acids: any role in rheumatoid arthritis? Lipids Health Dis. 16 (2017) 197, https://doi.org/10.1186/s12944-017-0586-3.

[9] S.M. Proudman, M.J. James, L.D. Spargo, R.G. Metcalf, T.R. Sullivan, M. Rischmueller, K. Flabouris, M.D. Wechalekar, A.T. Lee, L.G. Cleland, Fish oil in recent onset rheumatoid arthritis: a randomised, double-blind controlled trial within algorithm-based drug use, Ann. Rheum. Dis. 74 (2015) 89–95, https://doi.org/10.1136/annrheumdis-2013-204145.

[10] S. Adams, A.L. Lopata, C.M. Smuts, R. Baatjies, M.F. Jeebhay, Relationship between serum omega-3 fatty acid and asthma endpoints, Int J Environ Res Public Health, 16, 2019, https://doi.org/10.3390/ijerph16010043.

[11] P.C. Calder, Omega-3 polyunsaturated fatty acids and inflammatory processes: nutrition or pharmacology? Br. J. Clin. Pharmacol. 75 (2013) 645–662, https://doi.org/10.1111/j.1365-2125.2012.04374.x.

[12] F. Zapata-Gonzalez, F. Rueda, J. Petriz, P. Domingo, F. Villarroya, J. Diaz-Delfin, M.A. de Madariaga, J.C. Domingo, Human dendritic cell activities are modulated by the omega-3 fatty acid, docosahexaenoic acid, mainly through PPARγ:RXR heterodimers: comparison with other polyunsaturated fatty acids, J. Leukoc. Biol. 84 (2008) 1172–1182, https://doi.org/10.1189/jlb.1007688.

[13] K. Nakamoto, K. Shimada, S. Harada, Y. Morimoto, A. Hirasawa, S. Tokuyama, DHA supplementation prevent the progression of NASH via GPR120 signaling, Eur. J. Pharmacol. 820 (2018) 31–38, https://doi.org/10.1016/j.ejphar.2017.11.046.

[14] D.Y. Oh, S. Talukdar, E.J. Bae, T. Imamura, H. Morinaga, W. Fan, P. Li, W.J. Lu, S. M. Watkins, J.M. Olefsky, GPR120 is an omega-3 fatty acid receptor mediating potent anti-inflammatory and insulin-sensitizing effects, Cell 142 (2010) 687–698, https://doi.org/10.1016/j.cell.2010.07.041.

[15] M.G.J. Balvers, K.C.M. Verhoeckx, S. Bijlsma, C.M. Rubingh, J. Meijerink, H. M. Wortelboer, R.F. Witkamp, Fish oil and inflammatory status alter the n-3 to n-6 balance of the endocannabinoid and oxylipin metabolomes in mouse plasma and tissues, Metabolomics 8 (2012) 1130–1147, https://doi.org/10.1007/s11306-012-0421-9.

[16] P.C. Calder, Marine omega-3 fatty acids and inflammatory processes: effects, mechanisms and clinical relevance, Biochim. Biophys. Acta Mol. Cell Biol. Lipids 1851 (2015) 469–484, https://doi.org/10.1016/j.bbalip.2014.08.010.

[17] P.C. Calder, Omega-3 fatty acids and inflammatory processes: from molecules to man, Biochem. Soc. Trans. 45 (2017) 1105–1115, https://doi.org/10.1042/BST20160474.

[18] C.N. Serhan, N. Chiang, T.E. Van Dyke, Resolving inflammation: dual anti-inflammatory and pro-resolution lipid mediators, Nat. Rev. Immunol. 8 (2008) 349–361, https://doi.org/10.1038/nri2294.

[19] C.N. Serhan, B.D. Levy, Resolvins in inflammation: emergence of the pro-resolving superfamily of mediators, J. Clin. Investig. 128 (2018) 2657–2669, https://doi.org/10.1172/JCI97943.

[20] M.G.J. Balvers, H.M. Wortelboer, R.F. Witkamp, K.C.M. Verhoeckx, Liquid chromatography–tandem mass spectrometry analysis of free and esterified fatty acid N-acyl ethanolamines in plasma and blood cells, Anal. Biochem. 434 (2013) 275–283, https://doi.org/10.1016/j.ab.2012.11.008.

[21] T. Bisogno, I. Delton-Vandenbroucke, A. Milone, M. Lagarde, V. Di Marzo, Biosynthesis and inactivation of N-arachidonoylethanolamine (Anandamide) and N-docosahexaenoylethanolamine in bovine retina, Arch. Biochem. Biophys. 370 (1999) 300–307, https://doi.org/10.1006/abbi.1999.1410.

[22] J.T. Wood, J.S. Williams, L. Pandarinathan, D.R. Janero, C.J. Lammi-Keefe, A. Makriyannis, Dietary docosahexaenoic acid supplementation alters select physiological endocannabinoid-system metabolites in brain and plasma, J Lipid Res., 51 (2010) 1416–1423.doi:10.1194%2Fjlr.M002436.

[23] A.C. Kendall, S.M. Pilkington, K.A. Massey, G. Sassano, L.E. Rhodes, A. Nicolaou, Distribution of bioactive lipid mediators in human skin, J. Invest. Dermatol. 135 (2015) 1510–1520, https://doi.org/10.1038/jid.2015.41.

[24] V. Kantae, S. Ogino, M. Noga, A.C. Harms, R.M. van Dongen, G.L.J. Onderwater, A. M.J.M. van den Maagdenberg, G.M. Terwindt, M. van der Stelt, M.D. Ferrari, T. Hankemeier, Quantitative profiling of endocannabinoids and related N-

acylethanolamines in human CSF using nano LC-MS/MS, J. Lipid Res. 58 (2017) 615–624, https://doi.org/10.1194/jlr.d070433.
[25] J. Czepiel, J. Gdula-Argasińska, G. Biesiada, B. Bystrowska, A. Jurczyszyn, W. Perucki, K. Sroczyńska, A. Zając, T. Librowski, A. Garlicki, Fatty acids and selected endocannabinoids content in cerebrospinal fluids from patients with neuroinfections, Metab. Brain Dis. 34 (2019) 331–339, https://doi.org/10.1007/s11011-018-0347-7.
[26] M.G.J. Balvers, K.C.M. Verhoeckx, J. Meijerink, S. Bijlsma, C.M. Rubingh, H. M. Wortelboer, R.F. Witkamp, Time-dependent effect of in vivo inflammation on eicosanoid and endocannabinoid levels in plasma, liver, ileum and adipose tissue in C57BL/6 mice fed a fish-oil diet, Int. Immunopharmacol. 13 (2012) 204–214, https://doi.org/10.1016/j.intimp.2012.03.022.
[27] E. Leishman, K. Mackie, S. Luquet, H.B. Bradshaw, Lipidomics profile of a NAPE-PLD KO mouse provides evidence of a broader role of this enzyme in lipid metabolism in the brain, Biochim. Biophys. Acta Mol. Cell Biol. Lipids 1861 (2016) 491–500, https://doi.org/10.1016/j.bbalip.2016.03.003.
[28] H.-Y. Kim, A.A. Spector, N-docosahexaenoylethanolamine: a neurotrophic and neuroprotective metabolite of docosahexaenoic acid, Mol. Asp. Med. 64 (2018) 34–44, https://doi.org/10.1016/j.mam.2018.03.004.
[29] J. Meijerink, M.G.J. Balvers, R.F. Witkamp, N-acyl amines of docosahexaenoic acid and other n–3 polyunsatured fatty acids – from fishy endocannabinoids to potential leads, Br. J. Pharmacol. 169 (2013) 772–783, https://doi.org/10.1111/bph.12030.
[30] T. Park, H. Chen, H.-Y. Kim, GPR110 (ADGRF1) mediates anti-inflammatory effects of N-docosahexaenoylethanolamine, J. Neuroinflammation 16 (2019) 225, https://doi.org/10.1186/s12974-019-1621-2.
[31] M.G.J. Balvers, K.C.M. Verhoeckx, P. Plastina, H.M. Wortelboer, J. Meijerink, R. F. Witkamp, Docosahexaenoic acid and eicosapentaenoic acid are converted by 3T3-L1 adipocytes to N-acyl ethanolamines with anti-inflammatory properties, Biochim. Biophys. Acta Mol. Cell Biol. Lipids 1801 (2010) 1107–1114, https://doi.org/10.1016/j.bbalip.2010.06.006.
[32] J. Meijerink, P. Plastina, J.-P. Vincken, M. Poland, M. Attya, M. Balvers, H. Gruppen, B. Gabriele, R.F. Witkamp, The ethanolamide metabolite of DHA, docosahexaenoylethanolamine, shows immunomodulating effects in mouse peritoneal and RAW264.7 macrophages: evidence for a new link between fish oil and inflammation, Br. J. Nutr., 105 (2011) 1798–1807.doi:https://doi.org/10.1017/S0007114510005635.
[33] J. Meijerink, M. Poland, M.G.J. Balvers, P. Plastina, C. Lute, J. Dwarkasing, K. van Norren, R.F. Witkamp, Inhibition of COX-2-mediated eicosanoid production plays a major role in the anti-inflammatory effects of the endocannabinoid N-docosahexaenoylethanolamine (DHEA) in macrophages, Br. J. Pharmacol. 172 (2015) 24–37, https://doi.org/10.1111/bph.12747.
[34] R. Witkamp, Fatty acids, endocannabinoids and inflammation, Eur. J. Pharmacol. 785 (2016) 96–107, https://doi.org/10.1016/j.ejphar.2015.08.051.
[35] R. Yang, G. Fredman, S. Krishnamoorthy, N. Agrawal, D. Irimia, D. Piomelli, C. N. Serhan, Decoding functional metabolomics with docosahexaenoyl ethanolamide (DHEA) identifies novel bioactive signals, J. Biol. Chem. 286 (2011) 31532–31541, https://doi.org/10.1074/jbc.m111.237990.
[36] D.R. McDougle, J.E. Watson, A.A. Abdeen, R. Adili, M.P. Caputo, J.E. Krapf, R. W. Johnson, K.A. Kilian, M. Holinstat, A. Das, Anti-inflammatory ω-3 endocannabinoid epoxides, Proc. Natl. Acad. Sci. U. S. A. 114 (2017) E6034–E6043, https://doi.org/10.1073/pnas.1610325114.
[37] J. Roy, J.E. Watson, I.S. Hong, T.M. Fan, A. Das, Antitumorigenic properties of omega-3 endocannabinoid epoxides, J. Med. Chem. 61 (2018) 5569–5579, https://doi.org/10.1021/acs.jmedchem.8b00243.
[38] I. de Bus, H. Zuilhof, R. Witkamp, M. Balvers, B. Albada, Novel COX-2 products of n-3 polyunsaturated fatty acid-ethanolamine-conjugates identified in RAW 264.7 macrophages, J Lipid Res., (2019).doi:10.1194%2Fjlr.M094235.
[39] K. Lin, H. Kools, P.J. de Groot, A.K. Gavai, R.K. Basnet, F. Cheng, J. Wu, X. Wang, A. Lommen, G.J. Hooiveld, G. Bonnema, R.G. Visser, M.R. Muller, J.A. Leunissen, MADMAX - management and analysis database for multiple ~omics experiments, J Integr Bioinform 8 (2011) 160, https://doi.org/10.1515/jib-2011-160.
[40] R.A. Irizarry, B. Hobbs, F. Collin, Y.D. Beazer-Barclay, K.J. Antonellis, U. Scherf, T. P. Speed, Exploration, normalization, and summaries of high density oligonucleotide array probe level data, Biostatistics (Oxford, England), 4 (2003) 249–264.doi:https://doi.org/10.1093/biostatistics/4.2.249.
[41] B.S. Carvalho, R.A. Irizarry, A framework for oligonucleotide microarray preprocessing, Bioinformatics (Oxford, England), 26 (2010) 2363–2367.doi:https://doi.org/10.1093/bioinformatics/btq431.
[42] M. Dai, P. Wang, A.D. Boyd, G. Kostov, B. Athey, E.G. Jones, W.E. Bunney, R. M. Myers, T.P. Speed, H. Akil, S.J. Watson, F. Meng, Evolving gene/transcript definitions significantly alter the interpretation of GeneChip data, Nucleic Acids Res. 33 (2005), e175, https://doi.org/10.1093/nar/gni179.
[43] B.M. Bolstad, R.A. Irizarry, M. Astrand, T.P. Speed, A comparison of normalization methods for high density oligonucleotide array data based on variance and bias, Bioinformatics (Oxford, England), 19 (2003) 185–193.doi:https://doi.org/10.1093/bioinformatics/19.2.185.
[44] M.A. Sartor, C.R. Tomlinson, S.C. Wesselkamper, S. Sivaganesan, G.D. Leikauf, M. Medvedovic, Intensity-based hierarchical Bayes method improves testing for differentially expressed genes in microarray experiments, BMC Bioinform. 7 (2006) 538, https://doi.org/10.1186/1471-2105-7-538.
[45] G.K. Smyth, Linear models and empirical bayes methods for assessing differential expression in microarray experiments, Stat Appl Genet Mol Biol, 3, 2004, https://doi.org/10.2202/1544-6115.1027.
[46] M.E. Ritchie, D. Diyagama, J. Neilson, R. van Laar, A. Dobrovic, A. Holloway, G. K. Smyth, Empirical array quality weights in the analysis of microarray data, BMC Bioinform. 7 (2006) 261, https://doi.org/10.1186/1471-2105-7-261.
[47] R. Liu, A.Z. Holik, S. Su, N. Jansz, K. Chen, H.S. Leong, M.E. Blewitt, M.L. Asselin-Labat, G.K. Smyth, M.E. Ritchie, Why weight? Modelling sample and observational level variability improves power in RNA-seq analyses, Nucleic Acids Res. 43 (2015), e97, https://doi.org/10.1093/nar/gkv412.
[48] W.A. Schroder, T.D. Hirata, T.T. Le, J. Gardner, G.M. Boyle, J. Ellis, E. Nakayama, D. Pathirana, H.I. Nakaya, A. Suhrbier, SerpinB2 inhibits migration and promotes a resolution phase signature in large peritoneal macrophages, Sci. Rep. 9 (2019), 12421, https://doi.org/10.1038/s41598-019-48741-w.
[49] J.E. McDermott, K.B. Vartanian, H. Mitchell, S.L. Stevens, A. Sanfilippo, M. P. Stenzel-Poore, Identification and validation of Ifit1 as an important innate immune bottleneck, PLoS One 7 (2012), e36465, https://doi.org/10.1371/journal.pone.0036465.
[50] J. Ge, Y. Wang, Y. Feng, H. Liu, X. Cui, F. Chen, G. Tai, Z. Liu, Direct effects of activin A on the activation of mouse macrophage RAW264.7 cells, Cell Mol Immunol 6 (2009) 129–133, https://doi.org/10.1038/cmi.2009.18.
[51] Y.-C. Lu, W.-C. Yeh, P.S. Ohashi, LPS/TLR4 signal transduction pathway, Cytokine 42 (2008) 145–151, https://doi.org/10.1016/j.cyto.2008.01.006.
[52] F. Schmitz, J. Mages, A. Heit, R. Lang, H. Wagner, Transcriptional activation induced in macrophages by Toll-like receptor (TLR) ligands: from expression profiling to a model of TLR signaling, Eur. J. Immunol. 34 (2004) 2863–2873, https://doi.org/10.1002/eji.200425228.
[53] D.S. Shouval, J. Ouahed, A. Biswas, J.A. Goettel, B.H. Horwitz, C. Klein, A. M. Muise, S.B. Snapper, Interleukin 10 receptor signaling: master regulator of intestinal mucosal homeostasis in mice and humans, Adv. Immunol. 122 (2014) 177–210, https://doi.org/10.1016/B978-0-12-800267-4.00005-5.
[54] R.-B. Ding, J. Bao, C.-X. Deng, Emerging roles of SIRT1 in fatty liver diseases, Int J Biol Sci, 13 (2017) 852–867.doi:10.7150%2Fijbs.19370.
[55] M. Johnson, The anti-inflammatory profile of fluticasone propionate, Allergy 50 (1995) 11–14, https://doi.org/10.1111/j.1398-9995.1995.tb02735.x.
[56] M. Poland, J.P. ten Klooster, Z. Wang, R. Pieters, M. Boekschoten, R. Witkamp, J. Meijerink, Docosahexaenoyl serotonin, an endogenously formed n-3 fatty acid-serotonin conjugate has anti-inflammatory properties by attenuating IL-23–IL-17 signaling in macrophages, Biochim. Biophys. Acta Mol. Cell Biol. Lipids 1861 (2016) 2020–2028, https://doi.org/10.1016/j.bbalip.2016.09.012.
[57] Y. Wang, P. Plastina, J.-P. Vincken, R. Jansen, M. Balvers, J.P. ten Klooster, H. Gruppen, R. Witkamp, J. Meijerink, N-docosahexaenoyl dopamine, an endocannabinoid-like conjugate of dopamine and the n-3 fatty acid docosahexaenoic acid, attenuates lipopolysaccharide-induced activation of microglia and macrophages via COX-2, ACS Chem. Neurosci. 8 (2017) 548–557, https://doi.org/10.1021/acschemneuro.6b00298.
[58] D.M. Ojcius, A. Jafari, L. Yeruva, C.W. Schindler, A.A. Abdul-Sater, Dicer regulates activation of the NLRP3 inflammasome, PLoS One 14 (2019) e0215689, https://doi.org/10.1371/journal.pone.0215689.
[59] Z. Zhong, S. Liang, E. Sanchez-Lopez, F. He, S. Shalapour, X.-j. Lin, J. Wong, S. Ding, E. Seki, B. Schnabl, A.L. Hevener, H.B. Greenberg, T. Kisseleva, M. Karin, New mitochondrial DNA synthesis enables NLRP3 inflammasome activation, Nature 560 (2018) 198–203, https://doi.org/10.1038/s41586-018-0372-z.
[60] P. Pelegrin, C. Barroso-Gutierrez, A. Surprenant, P2X7 receptor differentially couples to distinct release pathways for IL-1β in mouse macrophage, J. Immunol. 180 (2008) 7147–7157, https://doi.org/10.4049/jimmunol.180.11.7147.
[61] G. Genard, S. Lucas, C. Michiels, Reprogramming of tumor-associated macrophages with anticancer therapies: radiotherapy versus chemo- and immunotherapies, Front. Immunol., 8 (2017).doi:https://doi.org/10.3389/fimmu.2017.00828.
[62] J. Sheng, Z. Xu, Three decades of research on angiogenin: a review and perspective, Acta Biochim. Biophys. Sin. 48 (2015) 399–410, https://doi.org/10.1093/abbs/gmv131.
[63] T. Park, H. Chen, K. Kevala, J.-W. Lee, H.-Y. Kim, N-docosahexaenoylethanolamine ameliorates LPS-induced neuroinflammation via cAMP/PKA-dependent signaling, J. Neuroinflammation 13 (2016) 284, https://doi.org/10.1186/s12974-016-0751-z.
[64] M. ten Hove, L. Pater, G. Storm, S. Weiskirchen, R. Weiskirchen, T. Lammers, R. Bansal, The hepatic lipidome: from basic science to clinical translation, Adv. Drug Deliv. Rev. (2020), https://doi.org/10.1016/j.addr.2020.06.027.
[65] K. Irungbam, Y. Churin, T. Matono, J. Weglage, M. Ocker, D. Glebe, M. Hardt, A. Koeppel, M. Roderfeld, E. Roeb, Cannabinoid receptor 1 knockout alleviates hepatic steatosis by downregulating perilipin 2, Lab. Investig. 100 (2020) 454–465, https://doi.org/10.1038/s41374-019-0327-5.
[66] M. Alhouayek, P. Bottemanne, A. Makriyannis, G.G. Muccioli, N-acylethanolamine-hydrolyzing acid amidase and fatty acid amide hydrolase inhibition differentially affect N-acylethanolamine levels and macrophage activation, Biochim. Biophys. Acta Mol. Cell Biol. Lipids 1862 (2017) 474–484, https://doi.org/10.1016/j.bbalip.2017.01.001.
[67] W.L. Smith, M.G. Malkowski, Interactions of fatty acids, nonsteroidal anti-inflammatory drugs, and coxibs with the catalytic and allosteric subunits of cyclooxygenases-1 and -2, J. Biol. Chem., 294 (2019) 1697–1705.doi:10.1074%2Fjbc.TM118.006295.
[68] Neser Unver, Gunes Esendagli, Guldal Yilmaz, Dicle Guc, CXCL7-induced macrophage infiltration in lung tumor is independent of CXCR2 expression CXCL7-induced macrophage chemotaxis in LLC tumors, Cytokine 75 (2) (2015) 330–337, https://doi.org/10.1016/j.cyto.2015.07.018.